Food Chemistry 492 (2025) 145618

Contents lists available at ScienceDirect

Food Chemistry

journal homepage: www.elsevier.com/locate/foodchem

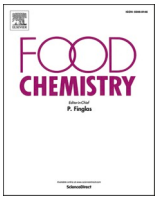

Ulvan as a source of oligosaccharides for biological applications: enzymatic hydrolysis in a biocompatible medium

Beatrice Zonfrillo [a], Maria Bellumori [a], Eleonora Truzzi [b], Mohamad Khatib [a], Paola Faraoni [c], Davide Bertelli [b], Francesco Ranaldi [c], Nadia Mulinacci [a,*]

[a] Department of Neuroscience, Psychology, Drug Research and Child Health (NEUROFARBA), University of Florence, via Ugo Schiff 6, Sesto Fiorentino, Italy
[b] Department of Life Science, University of Modena-Reggio Emilia, Via Campi 103, Modena, Italy
[c] Department of Experimental and Clinical Biomedical Sciences "Mario Serio", University of Florence, Viale Pieraccini 6, Florence, Italy

ARTICLE INFO

Keywords:
Ulva lactuca
Sea lettuce
Uronic acids
NMR-DOSY
UHPLC-MS/MS
ulvan lyase PLSV_3875

ABSTRACT

Ulvan oligosaccharides, which exhibit greater solubility than high molecular weight ulvan, hold significant potential for the valorization of *Ulva* biomass. They have been shown to promote the growth of probiotic bacteria in fermentation models and have demonstrated protective and anti-inflammatory effects in animal models.

The enzymatic hydrolysis of ulvan using the commercial ulvan lyase PLSV_3875 bypasses the challenge posed by the resistance of ulvanobiuronic acids to conventional acidic hydrolysis. This study aimed to develop a rapid, scalable, and efficient method for a complete ulvan hydrolysis under reduced salt concentrations, yielding oligosaccharides suitable for biological applications. The enzyme's robustness and kinetic parameters were evaluated. Enzyme activity was assessed at pH 6–10.5 with 0–100 mM Tris-HCl, carbonate or phosphate buffer, and 0–200 mM NaCl/KCl. Optimal conditions were identified as 3 mg/mL ulvan, 25 mM KCl, and 100 mM phosphate buffer at pH 7.5. The resulting oligosaccharides were characterized using 2D-NMR and UHPLC-MS/MS.

1. Introduction

Ulva lactuca L. (sea lettuce) is a green macroalga of the Ulvaceae family, widely distributed across marine ecosystems. Its rapid proliferation, exacerbated by water eutrophication, often leads to "green tides" (Hayden et al., 2003; Wichard, 2023). Despite these ecological concerns, *Ulva* species have been utilized as food and feed, with *U. lactuca* officially included in the EU's list of authorized algae for food and dietary supplements (Araújo & Peteiro, 2021). Among the bioactive compounds of sea lettuce, the sulfated polysaccharide ulvan – constituting 9–36% of the algal dry weight – is characteristic of this genus and the most interesting one (Liu et al., 2022).

Ulvan consists of repeating disaccharide units linked by α- or β-glycosidic bonds, primarily type A_{3S} (α-L-rhamnose-3-sulfate – Rha3S, linked to β-D-glucuronic acid - GlcA), along with minor units with Rha3S connected to α-L-iduronic acid – IdoA (type B_{3S}), β-D-xylose - Xyl (type U_{3S}), or β-D-xylose-2-sulfate ($U_{2,S3S}$) (Kidgell et al., 2019). It has been employed in food formulations, such as a synbiotic yogurt, in which ulvan acts as both a prebiotic ingredient, promoting the growth of probiotic bacteria, and as a viscosity and firmness enhancer (Shalaby & Amin, 2019). In addition, its unique sugar composition, degree of sulfation, and molecular weight (MW) have been linked to a range of biological activities, including antioxidant, anti-inflammatory, immunomodulatory, and anti-hyperlipidemic properties (Liu et al., 2022). However, its low water solubility (Chiellini & Morelli, 2011) limits the applicability of ulvan, making low MW ulvan promising alternatives for the development of functional food or dietary supplements with prebiotic properties (C. Li et al., 2023). These oligosaccharides have been shown to promote the growth of beneficial probiotic strains of *Lactobacillus acidophilus* and *L. bulgaricus* (Jagtap et al., 2022), as well as show protective and hypoglycemic effects in in vivo models of intestinal inflammation (Li, Ye, et al., 2020) and diabetes (Chen et al., 2022).

Ulvan is generally a long and linear polymer (Kidgell et al., 2024), and the production of its oligosaccharides requires hydrolytic steps following extraction. Chemical hydrolysis methods, such as acid hydrolysis (e.g., HCl or H_2SO_4) (J. Li et al., 2017) or ion-exchange resin

Abbreviations: GlcA, glucuronic acid; IdoA, iduronic acid; Rha, rhamnose; Xyl, xylose; Δ, 4-deoxy-L-threo-hex-4-enopyranosiduronic acid.

* Corresponding author at: Department of Neuroscience, Psychology, Drug Research and Child Health (NEUROFARBA), University of Florence, Via Ugo Schiff 6, Sesto Fiorentino, Italy.
E-mail address: nadia.mulinacci@unifi.it (N. Mulinacci).

https://doi.org/10.1016/j.foodchem.2025.145618
Received 12 February 2025; Received in revised form 17 July 2025; Accepted 19 July 2025
Available online 21 July 2025

depolymerization (e.g., Amberlite FPC23) (Adrien et al., 2019; Fournière et al., 2019) have been used to produce low MW ulvan, but they lack control over polymerization degree and often cause sulfate loss and unwanted degradation (Flórez-Fernández et al., 2023). Oxidative depolymerization with hydrogen peroxide offers an alternative but can lead to variable yields and partial desulfation (Baltrusch et al., 2024; Flórez-Fernández et al., 2023). Moreover, ulvan contains ulvanobiuronic acid linkages, which are resistant to conventional acid hydrolysis, often requiring prolonged reaction times that favor degradation (Baltrusch et al., 2024; De Ruiter et al., 1992), thus limiting a controlled and reproducible production of oligosaccharides suitable for food or biomedical applications.

To overcome these limitations, enzymatic hydrolysis using ulvan lyases (EC 4.2.2.-) is preferred. This method operates under mild conditions, enables selective cleavage of ulvan's glycosidic bonds, and ensures the production of oligosaccharides with defined structures while preserving functional groups, thus offering higher efficiency and suitability for food-grade applications (Ning et al., 2022). These enzymes catalyze the endolytic cleavage of glycosidic bonds between Rha3S and uronic acids through a β-elimination reaction, generating a reducing rhamnose end and an unsaturated 4-deoxy-L-threo-hex-4-enopyranosiduronic acid (Δ) (Fig. 1) (Li, Hu, et al., 2020).

Several ulvan lyases have been identified in marine bacteria (*Alteromonas* sp., *Pseudoalteromonas* sp., *Formosa agariphila*, *Glaciecola*, *Catenovulum maritimum*, *Nonlabens ulvanivorans*) and in the gut microbiota of marine animals. Based on sequence homology, they are classified into five polysaccharide lyase (PL) families in the Carbohydrate-Active enZymes (CAZy) database: PL24, PL25, PL28, PL37, and PL40 (Lombard et al., 2014). Among them, PL24 ulvan lyases specifically cleave Rha3S-GlcA linkages, while others act on both Rha3S-GlcA and Rha3S-IdoA residues (Konasani et al., 2018).

As ulvan lyases are marine enzymes, they typically work under alkaline conditions (pH 8.2–8.5) and in the presence of high NaCl concentration, reflecting their natural environment, while their optimal temperatures generally range between 30 and 50 °C (Rodrigues et al., 2024; Tang et al., 2021) (Table S1). Their activity is strongly influenced by temperature, pH, ionic strength, and metal ions (Tang et al., 2021), therefore, despite their similarities in structure and mechanism, each enzyme exhibits distinct kinetic properties and requires specific environmental conditions for optimal performance.

Among the commercially available ulvan lyases, PLSV_3875 (59.6 kDa) of PL24 family, firstly isolated by Kopel et al. (2016) from *Pseudoalteromonas* sp. PLSV, is characterized by superior thermal stability, retaining 100% activity after 24 h at 30 °C. While recent studies on PL24 ulvan lyases have characterized their pH dependence, medium composition, temperature, and kinetic properties (Rodrigues et al., 2024; Xu et al., 2021) (Table S1), no efforts have been made to develop a more efficient and food-compatible hydrolysis protocol.

Based on this premise, this study aimed on developing a rapid and efficient protocol to produce oligosaccharides suitable for food and biological application, with potential for scale-up and without the need for additional purification steps. In particular, the enzymatic hydrolysis of ulvan from *Ulva lactuca* L. was optimized using the commercially available ulvan lyase PLSV_3875. The work focused on overcoming the limitations of previous methodologies by reducing salt concentrations, adopting biocompatible reagents, and minimizing processing time and complexity. Furthermore, the oligosaccharides produced were characterized by one- and two-dimensional NMR and UHPLC-MS/MS analyses, and the robustness and kinetic parameters of the enzyme under optimized conditions were evaluated to support potential future applications.

2. Materials and methods

2.1. Reagents

The following reagents were purchased from Merck KGaA (Darmstadt, Germany): EtOH (#1.59010), HCl (#258148), NaOH (#567530), Tris-HCl (#T15760), Trizma® base (#252859), NaCl (#S9888), KCl (#P3911), KH_2PO_4 (#P0662), K_2CO_3 (#209619).

Deuterium oxide (D_2O, 99.9% atom % D), 3-(trimethylsilyl) propionic-2,2,3,3-d4 acid sodium salt (TSP), and sodium azide (NaN_3) were purchased from Sigma-Aldrich (Milan, Italy). Slide-A-Lyzer™ Dialysis Cassettes (10 K MWCO, #66830) were purchased from Thermo Fisher Scientific Inc. (Waltham, MA, USA). Recombinant ulvan lyase 24A (*P*Ulv24) from *Pseudoalteromonas* sp. PLSV_3875 (E.C. 4.2.2.-) was purchased from NZYtech Lda. (Lisbon, Portugal). Ultrapure water was obtained by the Milli-Q-system (Millipore SA, Molsheim, France).

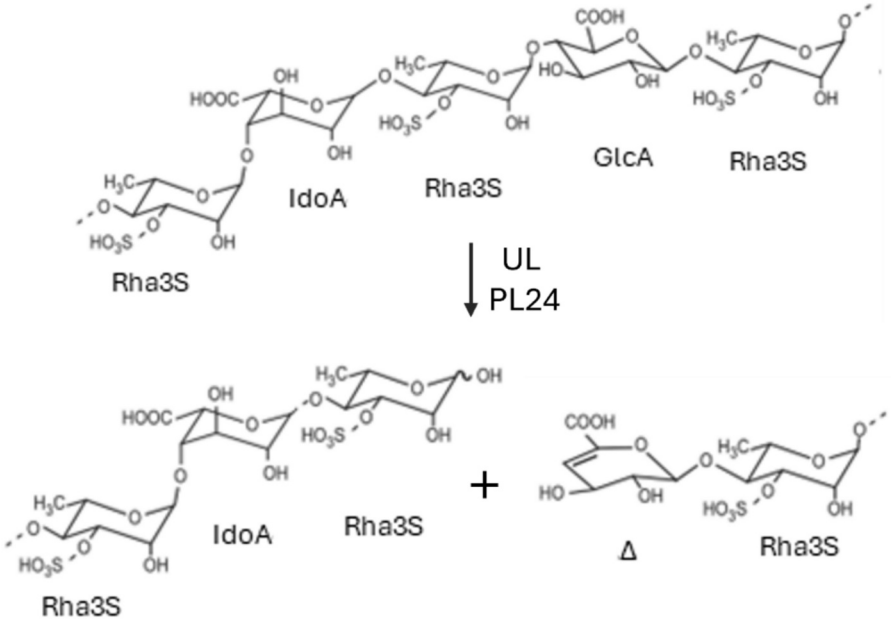

Fig. 1. Cleavage mechanism of ulvan lyases (UL) of PL24 family.

2.2. Ulvan extraction

Ulva lactuca was collected in August 2022 in the aquaculture tank of the Pescatori Orbetello cooperative in Tuscany (Italy). Ulvan was extracted with an optimized protocol recently published (Zonfrillo et al., 2025). Briefly, 10 g of dried algae was extracted with 600 mL of 0.01 M HCl under magnetic stirring (100 °C, 700 rpm, 105 min). Polysaccharides were precipitated by the addition of 3 volumes of EtOH, freeze-dried, dialyzed with 10 kDa cassette, and freeze-dried again. A detailed chemical characterization of ulvan in terms of structure, monosaccharide composition, sulfate content and molecular weight is reported in our previous work (Zonfrillo et al., 2025).

2.3. Ulvan lyase assays

All enzymatic assays were performed in multiwell-96 plates by an Infinite 200 Pro Tecan Plate Reader (AG, Switzerland), and the hydrolysis reaction was measured at 235 nm (an indication of the double bond formation after the β-elimination reaction).

Unless otherwise specified, all experiments were performed in triplicate at 30 °C with 1 mg/mL ulvan and 250 ng/mL ulvan lyase.

2.4. Different NaCl and Tris-HCl concentrations experiments

A complete factorial design was used to assess enzymatic activity with the recommended buffered medium (200 mM NaCl and 100 mM Tris-HCl, pH 7.5) and in a reduced presence of salts (0–12.5–25–50 - 100 mM NaCl, 0–6.25 - 12.5–25–50 - 100 mM Tris-HCl, pH 7.5). The activity of the enzyme was measured for 40 h.

2.5. Different pH and buffer solutions experiments

The influence of pH and different buffer solutions was evaluated in the following conditions: 25 and 50 mM NaCl; 100 mM Tris-HCl at pH 7.5–9.0; 100 mM phosphate buffer (KH_2PO_4/K_2HPO_4) at pH 6.0–7.5; 100 mM carbonate buffer ($KHCO_3/K_2CO_3$) at pH 9.0–10.5. One experiment for buffer series was also conducted with 25 and 50 mM KCl instead of NaCl.

2.6. Enzyme concentrations and kinetic measurements

Enzymatic activity was investigated for three concentrations of ulvan lyase (250, 150, and 50 ng/mL). The experiments were done in 25 mM KCl and 100 mM phosphate buffer at pH 7.5. The reaction was monitored for 4 h.

Michaelis-Menten plots were built using rate values of the ulvan hydrolysis reaction by ulvan lyase, determined at ulvan concentrations 0.01, 0.025, 0.05, 0.10, 0.25, 0.5, 1 mg/mL, in 100 mM phosphate buffer, pH 7.5, 25 mM KCl reaction mixture. The kinetic parameters, K_m and V_{max}, were calculated by directly fitting the data to the classical Michaelis-Menten equation using nonlinear regression. An extinction coefficient of 4800 M^{-1} cm^{-1} was used (Nyvall Collén et al., 2011; Rodrigues et al., 2024).

2.7. Enzyme robustness in relation to pH and temperature

The hydrolysis reaction was monitored before and after acidic, alkaline, freezing, and heating treatments for evaluation of enzyme stability.

For acidic treatments, 5% *v*/v HCOOH was added to the reaction mixture (25 mM KCl, 100 mM phosphate buffer, pH 7.5) after 12 min, and the reaction was monitored for another 20 min at 235 nm. The enzyme (10 μg/mL in 25 mM KCl, 100 mM phosphate buffer, pH 7.5) was also incubated for 1 h with HCOOH 5% without ulvan; then, an aliquot was mixed with the reaction mixture (ulvan 1 mg/mL, KCl 25 mM, 100 mM phosphate buffer, pH 7.5) to have final ulvan lyase concentration of 250 ng/mL. The reaction was monitored for 90 min at 235 nm.

For alkaline treatments, the enzyme (10 μg/mL in 25 mM KCl, 100 mM carbonate buffer, pH 10.5) was incubated for 1 h without ulvan. Then, an aliquot was mixed with the reaction medium (ulvan 1 mg/mL, KCl 25 mM, 100 mM phosphate buffer, pH 7.5) to achieve a final ulvan lyase concentration of 250 ng/mL. The reaction was monitored for 90 min at 235 nm.

For the freezing treatments, the reaction (25 mM KCl, 100 mM phosphate buffer, pH 7.5) was monitored for 5 min at 30 °C. Subsequently, the samples were stored for 24 h at −20 °C or − 80 °C or treated with liquid nitrogen. The frozen samples were defrosted, and the reaction was measured for 45 min at 235 nm.

For heating treatments, the enzyme (10 μg/mL) was placed in 25 mM KCl, 100 mM phosphate buffer, pH 7.5. After 10 min, the reaction was stopped by heating the samples for 10 min at 55, 75, or 95 °C. After heat treatments, the residual activity was monitored for 90 min at 235 nm.

2.8. NMR experiments

Ulvan, before hydrolysis, and the oligosaccharides produced were dissolved in D_2O solution containing TSP and NaN_3 and transferred into a WILMAD® NMR tube, 5 mm, Ultra-Imperial grade, 7 in. L,528-PP (Sigma-Aldrich, Milan, Italy). The NMR experiments were performed on a Bruker FT-NMR Avance III HD 600 MHz spectrometer equipped with a CryoProbe BBO H&F 5 mm (Bruker Biospin GmbH Rheinstetten, Karlsruhe, Germany). After loading the sample into the probe, 5 min was required to achieve thermal equilibrium. Afterward, the magnetic field was locked, and the probe head was tuned and matched. Finally, the sample was shimmed.

^1H, ^{13}C, ^1H—^1H COSY, ^1H—^{13}C HMBC, and ^1H—^{13}C HSQC experiments were performed for the structural characterization of the samples dissolved at the concentration of 12 mg/mL. The spectra were acquired, respectively, with the Bruker sequences “noesygppr1d” (D1, 8 s; pulse width, 12.22 μs; ns, 32), “zgpg_pisp_f2.fas” (D1, 5 s; pulse width, 11 μs; ns, 1048), “cosygpprqf” (D1, 1 s; pulse width, 12.22 μs; ns, 8), “hmbcetgpl3nd” (D1, 1 s; pulse width, 12.22; ns, 32), and “hsqcedetgpsp” (D1, 1.5 s; pulse width, 12.22 μs; ns 16). All experiments were conducted at 298 K. MestReNova 14.2.1 was used for baseline and phase corrections and chemical shift calibration according to the TSP signal.

Two-dimensional diffusion-ordered spectroscopy (DOSY) ^1H NMR experiments were performed on the original ulvan and the produced oligosaccharides dissolved in D_2O solution containing TSP and NaN_3 at the concentration of 3 mg/mL. DOSY ^1H NMR spectra were acquired using the standard Bruker “ledbpgp2s” pulse program using a longitudinal eddy current (LED) bipolar gradient pulse pair and two spoil gradients. Thirty-two gradient steps were used for the diffusion dimension from 2 to 95% of the linear gradient amplitude, where 65.7 G/cm was the maximum gradient intensity. Diffusion time (d20, Δ) and pulse field gradient length (P30, δ) were optimized for each sample and varied between 0.1 and 0.3 s and 750 and 2500 μs, respectively. For all the samples, the other acquisition parameters were set as follows: number of scans, 32; gradient strength (gpz6), 100%; LED delay (d21), 5 ms; total acquisition time was 1 h and 16 min. The DOSY spectra were processed via Bayesian method using Mnova® 14.1.2 software (Mestrelab Research) and the coefficient of diffusions (D) were determined. The molecular weight of the original ulvan was calculated by using the linear regression obtained by plotting the log(D) versus log(M_w) of six standard dextrans with molecular weights from 20 to 500 kDa (VWR International).

2.9. UHPLC-HRMS analysis

The hydrolysis products were analyzed on a Thermo Scientific (Waltham, MA, USA) UHPLC Ultimate 3000, equipped with a binary pump, a vacuum degasser, a thermostated autosampler, and column

compartment, and a Q-Exactive Orbitrap mass spectrometer, with a heated electrospray ionization (HESI) source. A hydrophilic interaction liquid chromatography was performed on a HILIC Cortecs UPLC column (1.6 μm, 2.1 × 100 mm). The mobile phase was composed of 20 mM ammonium formate in water (A) and 0.1% HCOOH in acetonitrile (B), and the gradient elution was set as follows: 0–1 min, 5% A; 1–11 min, 80% A; 11–20 min, 5% A; 20–45 min, 5% A. The flow rate was set at 0.3 mL/min, and the column temperature was maintained at 25 °C. MS acquisition was performed in negative ion mode. The source parameters were set as follows: sheath gas (N_2) 45, auxiliary gas (N_2) 25, sweep gas (N_2) 2, auxiliary gas temperature 290 °C, and electrospray voltage 3.40 kV (−). A data-dependent acquisition strategy was used to acquire both Full MS and higher energy collisional dissociation (HCD) fragmentation spectra. Mass analyzer acquisition parameters were set as follows: Full MS scan range 100 < *m/z* < 1500 at 35000 full-width half maximum (FWHM) resolving power with an automatic gain control (AGC) target set at 1×10^6 ions with 200 ms maximum injection time; Top 2 HCD fragmentation spectra of most abundant precursor ions were acquired at 17500FWHM resolving power using an isolation window of 1.0 *m/z* and stepped normalized collision energy (NCE) at 30.

2.10. Statistical analysis

One-way and two-way ANOVA, followed by Tukey post-hoc test, were performed in RStudio (2024.09.0 + 375). The activity (U/mL) was transformed by square root before the statistical analysis.

3. Results and discussion

A summary of the experimental workflow carried out in this study is presented in Fig. 2, outlining the key steps of hydrolysis optimization, kinetic characterization and oligosaccharide characterization. The hydrolysis optimization started considering the optimal conditions for PLSV_3875 reported by Kopel et al. (2016), namely 0.2 M NaCl and 0.1 M Tris-HCl of reaction medium, and 1 mg/mL ulvan. In this setup, ulvan represents only 3.5% *w*/w of the dried weight of the hydrolyzed sample, a concentration that is too low for future biological applications and potential large-scale production. Notably, the high NaCl concentration used for hydrolysis is unsuitable for food-related applications and may affect the prebiotic potential of ulvan oligosaccharides if used as substrates for evaluating this effect. The aim of the study was to overcome these limitations by choosing a more biocompatible medium to produce oligosaccharides from ulvan via an enzymatic hydrolysis.

3.1. Different NaCl and Tris-HCl concentrations experiments

The first phase of the study focused on evaluating the effects of reduced salt and buffer concentrations on enzymatic activity starting with the suggested conditions in literature (100 mM Tris-HCl and 200 mM NaCl) (Kopel et al., 2016) (Fig. 3).

A linear positive correlation was observed between enzyme activity (sqrt(U/mL)) and both NaCl and Tris-HCl concentrations, with regression coefficients (R^2) ranging from 0.77 to 1 (Fig. S1). The combined influence of these two variables was further evaluated using multiple linear regression. The resulting model was highly significant ($F(2,105) = 885$, $p < 2.2e\text{-}16$), explaining 94.4% of the overall variability in enzymatic activity (adjusted $R^2 = 0.943$). Regression coefficients indicate a positive relationship between both NaCl and Tris-HCl concentrations and sqrt(U/mL), as shown in Eq. 1 and Table S2.

$$y = 0.0232082 + 0.0043402x_1 + 0.0048423x_2 \quad (1)$$

where *y* is the enzymatic activity (sqrt(U/mL)), x_1 is NaCl concentration (mM) and x_2 is Tris-HCl concentration (mM).

As indicated by the higher slope (*m*) value, Tris-HCl influences the response slightly more than NaCl, although this difference is not statistically significant.

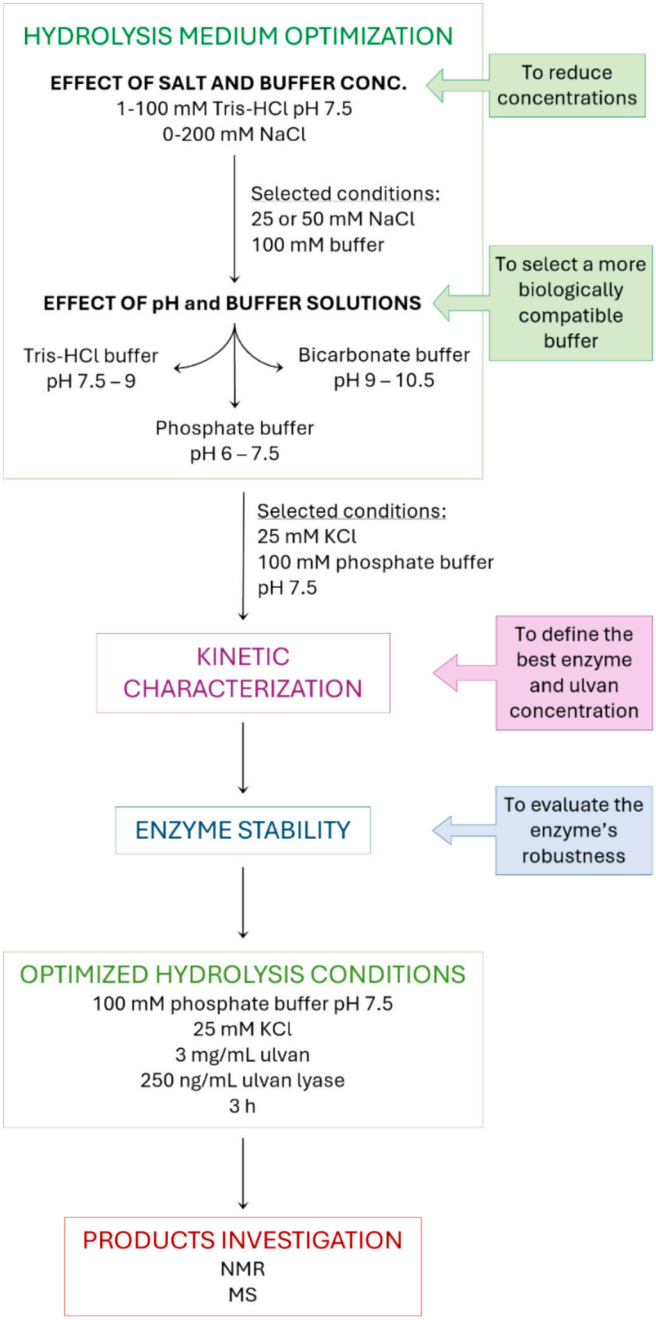

Fig. 2. Workflow of enzymatic hydrolysis optimization, kinetic characterization and chemical characterization of the produced oligosaccharides.

The results in Fig. 3 showed that, except for the experiments with the lowest values of NaCl and Tris-HCl, PLSV_3875 remained active even at low salt concentrations. This suggests that, given sufficient time, effective hydrolysis could still occur in most cases, as confirmed by the absorbance plateau of the reactions, which were monitored over 40 h (Table S3); even at NaCl concentration from 0 to 25 mM it was possible to reach 84% and 108% of the activity, respectively. The variation in maximum absorbance could be attributed either to enzyme instability over prolonged periods or to differences in the enzyme's affinity for ulvan, as previously reported for varying NaCl concentrations in *Fa*PL28 ulvan lyase (Reisky et al., 2018).

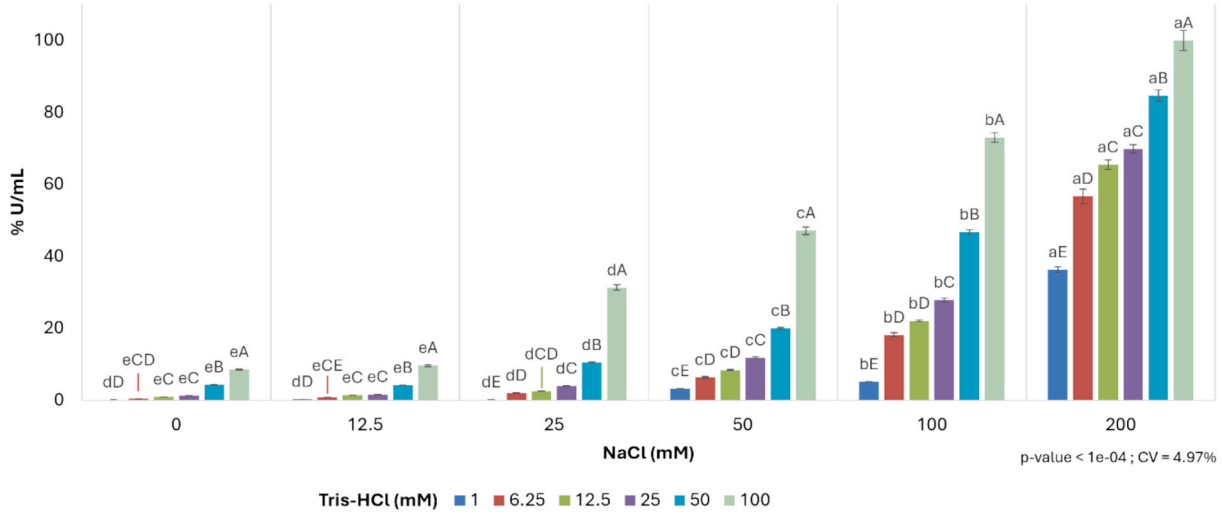

Fig. 3. Effects of NaCl and Tris-HCl on enzyme activity (U/mL); U is the enzyme amount that catalyzes the conversion of 1 μmol of substrate in 1 min. Data are means of triplicates and expressed as percentages relative to the activity measured at the recommended concentrations (200 mM NaCl, 100 mM Tris-HCl, pH 7.5) ± RSD (%). Statistically significant differences between Tris-HCl for each NaCl series and NaCl for each Tris-HCl series are indicated by different uppercase and lowercase letters, respectively ($p < 0.05$).

3.2. *Different pH and buffer solutions experiments*

The previous experiment demonstrated good activity values with low NaCl concentrations (25 and 50 mM) in the mixture, coupled with 100 mM Tris-HCl. These concentrations were, therefore, selected to assess the enzymatic activity under different pH conditions. To reach pH values higher and lower than 7.5, carbonate and phosphate buffers were used. Furthermore, more biologically compatible potassium buffers were

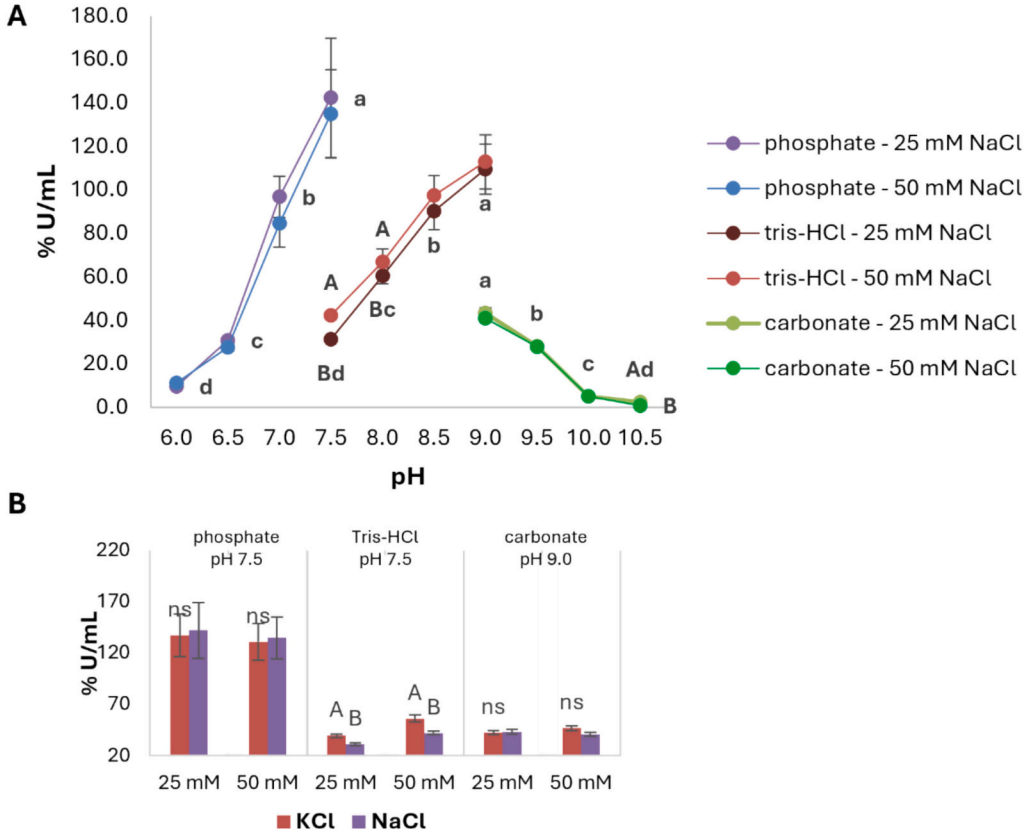

Fig. 4. Effect of pH and buffer composition on enzyme activity. **A**) Enzyme activity in different buffers across various pH values in the presence of NaCl. **B)** Comparison of NaCl and KCl effects on enzyme activity. Data represent the mean of triplicates, expressed as percentages relative to the activity at the recommended conditions (200 mM NaCl, 100 mM Tris-HCl, pH 7.5) ± RSD (%). In **A**, lowercase letters indicate statistically significant differences among pH values within each buffer series, while uppercase letters indicate significant differences between NaCl concentration within each buffer series and pH (2-way ANOVA followed by Tukey's post-hoc test, $p < 0.05$). In **B**, different uppercase letters indicate statistically significant differences between NaCl and KCl at the same concentration and pH (one-way ANOVA followed by Tukey's post-hoc test, $p < 0.05$).

preferred over sodium ones. The enzymatic activity varied significantly with pH and buffer type, highlighting the enzyme's robustness across a wide pH range (Fig. 4A). Activity was observed from pH 6.5 to 9, with the optimal pH differing by buffer: Tris-HCl at pH 9, phosphate at pH 7.5, and carbonate at pH 9. Differences between 25 and 50 mM NaCl were not significant, except in three cases where 50 mM NaCl yielded slightly higher activity. Tests with KCl showed similar or slightly higher results than those with NaCl, indicating the two salts could be used interchangeably (Fig. 4B).

Interestingly, the phosphate buffer produced notably high enzymatic activity – over four times greater than that with Tris-HCl at pH 7.5 ($F = 425.69$, $p < 0.001$, one-way ANOVA followed by Tukey's post-hoc test). This finding aligns with the results of Rodrigues et al. (2024) on the ulvan lyase from *Vibrio* FNV38, another member of the PL24 family, like PLSV_3875 used in this study. In contrast, ulvan lyases from *Alteromonas* sp. A321 (ALT_3695, of PL25 family) and *Formosa agariphila* KMM 3901^T (*Fa*PL28, PL28 family) have shown higher activity with Tris-HCl than with phosphate buffer (Gao et al., 2019; Reisky et al., 2018). This activity difference could be due to the ionic strength variation between the two buffers, as this parameter considers

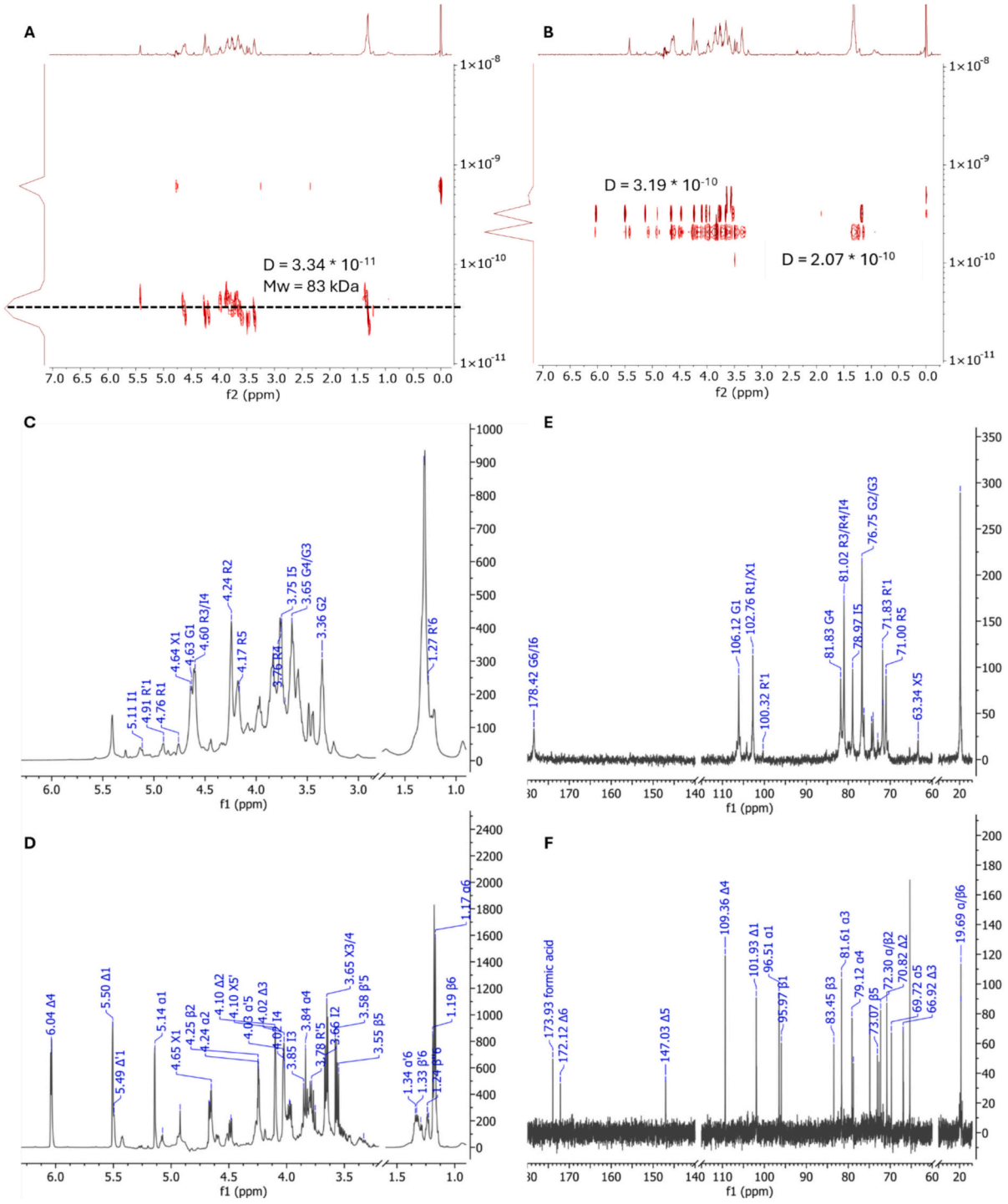

Fig. 5. DOSY spectra of **A)** original ulvan and **B)** hydrolyzed ulvan under optimized conditions. D, diffusion coefficient. ^{1}H NMR spectra of **C)** original ulvan and **D)** hydrolyzed ulvan. ^{13}C NMR spectra of **E)** original ulvan and **F)** hydrolyzed ulvan.

all charged species in solution and is strongly influenced by ion valence. However, ionic strength alone did not directly correlate with activity in our results (Fig. S2) but appeared to follow the same pH trend for each buffer series. Beyond ionic strength and pH – factors that affect the charge of amino acid lateral chains, enzyme conformation, and therefore activity – the specific ions themselves can play a significant role. The PO_4^{3-} ion appears to enhance PL24 ulvan lyase activity independently of pH and ionic strength. Although further investigation into this mechanism would be useful to understand the interaction at molecular level between PO_4^{3-} ion and ulvan lyase, it lies beyond the current study's scope.

Given these results and the frequent use of phosphate buffer in several biological assays, such as those focused on evaluating the fermentability of carbohydrates by human microbiota (Pérez-Burillo et al., 2021), phosphate buffer at pH 7.5 with 25 mM KCl was selected as the optimized hydrolysis medium for obtaining ulvan oligosaccharides.

3.3. Kinetics characterization

To characterize the enzyme's activity, a Michaelis-Menten plot was constructed under optimized reaction conditions using varying ulvan concentrations (Fig. S3). The analysis yielded a V_{max} of 2.4927 ± 0.1408 μM/min, a K_m of 0.1279 ± 0.0230 mg/mL, a k_{cat} of 9.87 s^{-1}, and a k_{cat}/K_m of 77.19 mL mg^{-1} s^{-1}. Compared to other PL24 family enzymes, the k_{cat} value obtained in this study is higher than those reported for PsPL from *Pseudoalteromonas* sp. strain PLSV (k_{cat} 7.08 ± 0.12 s^{-1}, K_m 2.10 ± 0.31 mg/mL, k_{cat}/K_m 3.37 mL mg^{-1} s^{-1}; reaction conditions: 100 mM Tris-HCl, 200 mM NaCl, pH 8, 100 μg/mL purified enzyme) (Qin et al., 2018) and AsPL from *Alteromonas* sp. (k_{cat} 4.19 ± 0.21 s^{-1}, K_m 3.19 ± 0.37 mg/mL, k_{cat}/K_m 1.31 mL mg^{-1} s^{-1}; reaction conditions: 20 mM Tris-HCl, 200 mM NaCl, pH 8.0, 100 μg/mL purified enzyme) (Qin et al., 2020).

In contrast, a higher k_{cat} value of 22.33 s^{-1} was reported by Rodrigues and coworkers for the PL24 enzyme from *Vibrio* sp. FNV38 (K_m 0.064 ± 0.002 mg/mL, k_{cat}/K_m 348.90 mL mg^{-1} s^{-1}; reaction conditions: 100 mM Tris-HCl, 600 mM NaCl, pH 8.5, 15 ng/mL purified enzyme) (Rodrigues et al., 2024). This latter case proposed a very high concentration of NaCl, three times higher than the maximum dose tested in this study.

The K_m value of the PLSV_3875 enzyme is significantly lower than those of PsPL and AsPL, aligning more closely with the K_m value of FNV38. Regarding catalytic efficiency (k_{cat}/K_m), PLSV_3875 exhibits higher efficiency than PsPL and AsPL, though it remains lower than that of FNV38. Notably, the reaction conditions proposed in this study employed significantly lower ionic strength, and thus reduced NaCl concentration, compared to those used in the comparative studies mentioned above, in particular for ulvan lyase from *Vibrio* sp. FNV38. This finding highlights the superior catalytic efficiency of the ulvan lyase PLSV_3875 under low-salt conditions, making it a promising candidate for applications where reduced salt is advantageous, such as the production of ulvan oligosaccharides for biological testing.

3.4. Optimization of enzyme and substrate concentrations

At an ulvan concentration of 1 mg/mL, the ulvan lyase PLSV_3875 already works at its maximum speed. Since increasing the ulvan concentration could enhance the process efficiency and decrease the relative weight of medium salts in the final hydrolyzed product, the ulvan concentration was increased to 3 mg/mL. Further increases were avoided as they interfered with the hydrolysis reaction due to the higher viscosity of the solution and the incomplete solubility of the ulvan (data not shown). However, this may not preclude the use of higher substrate concentrations in future scaled-up processes. A semi-suspension of ulvan could be employed, allowing a gradual solubilization as the reaction progresses. Such a strategy would extend reaction time but could reduce the costs per unit of product.

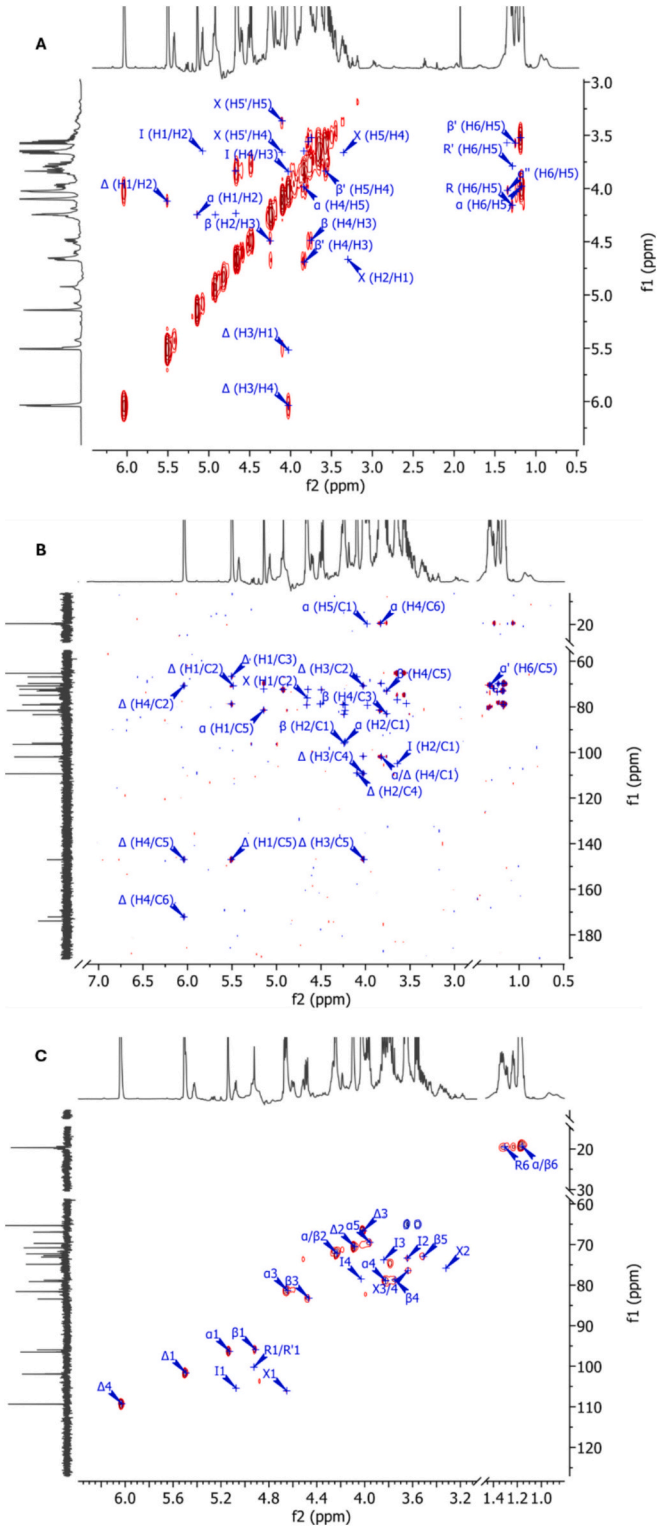

Fig. 6. 2D NMR spectra of hydrolyzed ulvan: **A)** $^{1}H—^{1}H$ COSY, **B)** $^{1}H—^{13}C$ HMBC, **C)** $^{1}H—^{13}C$ HSQC.

The effect of different enzyme concentrations was evaluated to improve hydrolysis efficiency under the optimized reaction conditions (100 mM phosphate buffer, pH 7.5, with 25 mM KCl). The enzyme activity was tested at lower concentrations of 150 and 50 ng/mL (Fig. S4). The results showed an excessive decrease in hydrolysis rate for the purpose of the study, which aimed to have a rapid hydrolytic process.

Table 1
^{1}H and ^{13}C chemical shifts of hydrolyzed ulvan.

Units	Acronym	Chemical shifts (ppm)					
		H1/ C1	H2/ C2	H3/ C3	H4/ C4	H5-H5'/ C5	H6/ C6
Disaccharide							
[D-ΔGlcA-(1→	Δ	5.50 101.93	4.10 70.82	4.02 66.92	6.04 109.36	147.03	172.12
4)-α-L-Rha3S]	α	5.14 96.51	4.23 72.30	4.67 81.61	3.84 79.12	3.98 69.72	1.17 19.69
4)-β-L-Rha3S]	β	4.92 95.97	4.25 72.30	4.48 83.45	3.75 78.78	3.55 73.07	1.19 19.69
Tetrasaccharide 1							
[D-ΔGlcA-(1→	Δ	5.49 101.93	4.10 70.82	4.10 66.92	6.04 109.36	147.03	172.12
4)-α-L-Rha3S-(1→	R	4.93 100.21				4.16 71.98	1.29 19.67
4)-β-D- Xyl-(1→	X	4.65 106.1	3.33 75.86	3.65 76.48	3.65 76.48	3.33/4.10 62.96	
4)-α-L- Rhap3S]	α'					4.01 70.54	1.34 19.64
4)-α-L- Rhap3S]	β'			4.49	3.79	3.55 73.58	1.33 19.69
Tetrasaccharide 2							
[D-ΔGlcA-(1→	Δ	5.50 101.93	4.10 70.82	4.02 66.92	6.04 109.36	147.03	172.12
4)-α-L-Rha3S-(1→	R'	4.93 100.21		4.49	3.56	3.78 71.98	1.29 19.67
4)-β-D-IdoA-(1→	I	5.08 105.40	3.65 73.38	3.84 73.79	4.03 78.50		
4)-α-L- Rhap3S]	α''					4.03 69.93	1.23 19.69
4)-α-L- Rhap3S]	β''					3.57 73.41	1.24 19.69

Under the reaction conditions here applied (25 mM KCl, 100 mM phosphate buffer, 3 mg/mL ulvan), the relative weight percentage of ulvan on the final dry extract increased by over 460%, from 3.5% to 16.2% *w*/w, compared to the initial conditions suggested by the literature (200 mM NaCl, 100 mM Tris-HCl, 1 mg/mL ulvan) (Kopel et al., 2016). At the same time, the co-present salts are typical constituent of media used for fermentation tests with human fecal samples (Pérez-Burillo et al., 2021).

3.5. Enzyme robustness

The use of the commercial ulvan lyase PLSV_3875 was chosen for this study to ensure reproducibility and guarantee a reliable supply of the enzyme with industrial-grade quality for possible future scale-up processes. Considering the potential use of the enzyme for preparative applications, PLSV_3875's robustness was tested in various storage conditions, thermal treatments, and pH values. The time/absorbance curves of these reactions are reported in Fig. S5. Acidic pH, obtained with 5% HCOOH added to the reaction solution, irreversibly inactivated the enzyme, halting the reaction and preventing reactivation even when pH was restored. In contrast, high alkaline pH only temporarily inhibited the enzyme's activity, which resumed once the pH returned to 7.5.

The enzyme remained stable and still active after storage at −20 and − 80 °C, as well as after snap freezing in liquid nitrogen (Fig. S5). Its activity during −20 °C storage was confirmed through preliminary experiments in Tris-HCl/NaCl buffer, in which partially hydrolyzed samples (collected after 4 h of hydrolysis) were stored at −20 °C for one week before lyophilization and NMR analysis. NMR-DOSY, a technique suitable to discriminate compounds based on their diffusion coefficient, which is proportional to their molecular weight/size, confirmed the production of oligosaccharides and the complete disappearance of the original ulvan peak (Fig. S6). Moreover, internal tests demonstrated that the enzyme remained stable for months at 4 °C, and even longer at −20 °C (data not shown). In contrast, heating treatments inactivated the enzyme at a relatively low temperature of 55 °C (Fig. S5), only slightly higher than the optimum temperature reported by Kopel et al. (2016). These results align with the enzyme's adaptation to its natural marine environment, where it encounters lower rather than higher temperatures.

In an industrial setting, the good storage stability of the enzyme may facilitate its reuse through recovery and recirculation strategies, thereby improving the cost-effectiveness of the process. Future developments could explore enzyme immobilization strategies—such as adsorption, covalent binding, or entrapment in polymeric matrices—which have been successfully applied to other glycoside hydrolases like those used in fructooligosaccharide production (Kumar et al., 2018). These systems enable repeated use and facilitate downstream processing and may be adapted to ulvan lyase in future scale-up processes.

3.6. Chemical characterization of the oligosaccharides

The production of oligosaccharides after the hydrolysis process was confirmed through NMR and MS experiments. DOSY analysis (Fig. 5A and B) of both original and hydrolyzed ulvan under optimized conditions demonstrated that, after 3 h of reaction, neither polysaccharide nor intermediate oligomers were detected in the hydrolyzed sample. Instead, two main peaks with diffusion coefficients of $3.19 * 10^{-10}$ and $2.07 * 10^{-10}$ were observed, significantly higher (by an order of magnitude) than the native ulvan's diffusion coefficient ($D = 3.34 * 10^{-11}$).

The ^{1}H NMR spectrum of hydrolyzed ulvan (Fig. 5D) showed two intense signals at 5.50 and 6.04 ppm, absent in the original ulvan spectrum (Fig. 5C). These signals were assigned to H1 and H4 of ΔGlcA,

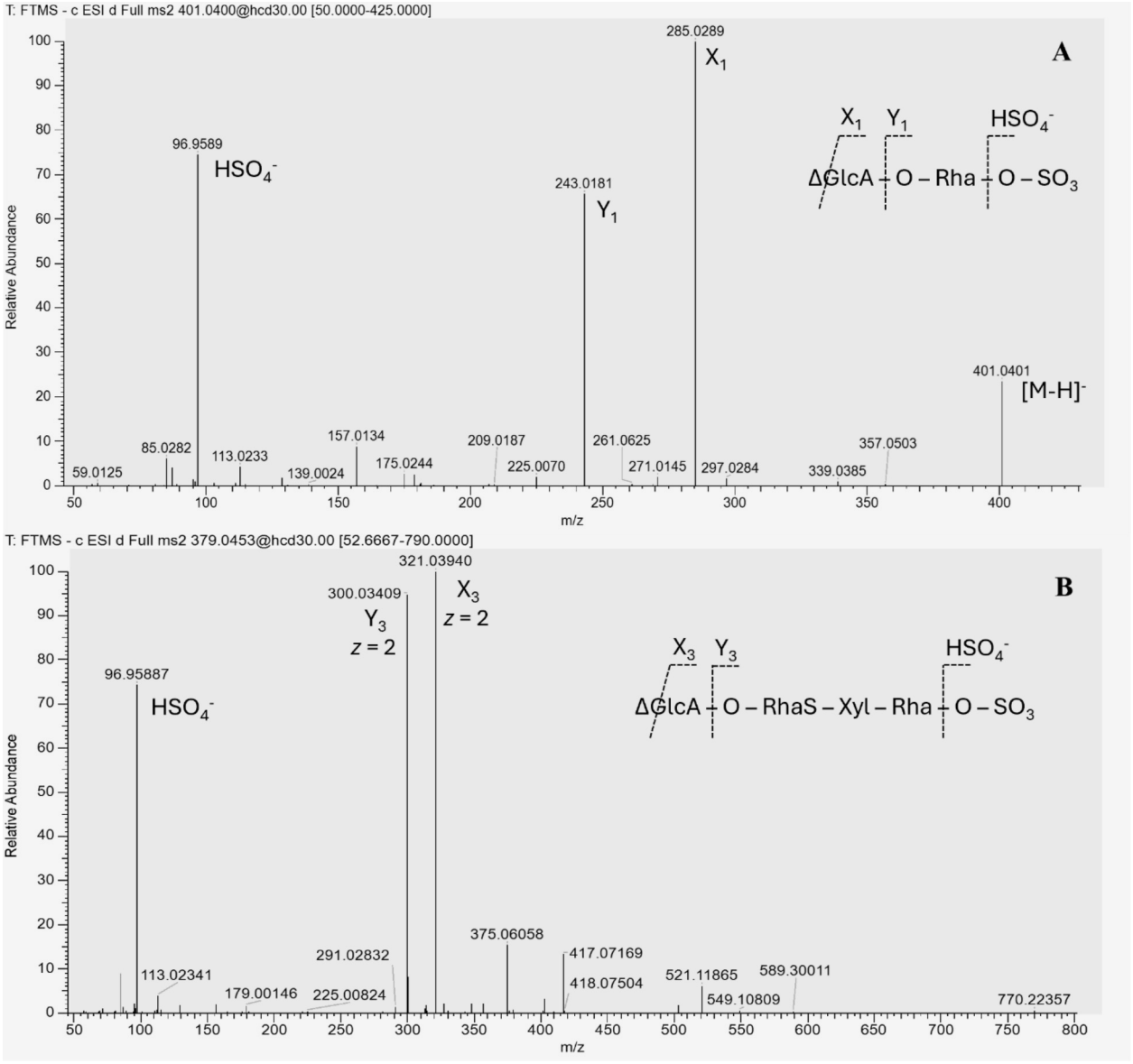

Fig. 7. MS^2 fragmentation spectra of the precursor ions at *m/z* 401.0400 **(A)** and 379.0453 **(B).**

consistent with literature data (Kopel et al., 2016). Additionally, a shift in the relative abundance of Rha H6 signals, originally around 1.30 ppm (bound Rha), toward anomeric free Rha-α/β (around 1.20 ppm) was observed. In ^{13}C spectra (Fig. 5E and F), signals corresponding to uronic acids largely disappeared in the hydrolyzed ulvan spectrum, while new peaks at 172.12 ppm (ΔGlcA C1) and 109.39 ppm (ΔGlcA C4) appeared.

Further structural characterization was performed through $^{1}H—^{1}H$ COSY, $^{1}H—^{13}C$ HMBC, and $^{1}H—^{13}C$ HSQC experiments (Fig. 6). Chemical shift assignments for ^{1}H and ^{13}C (Table 1) were based on literature references (Chi et al., 2020; Lahaye, 1998). Starting from the characteristic proton signal at 5.50 ppm, six ^{1}H resonances were identified from in the COSY spectrum (Fig. 6A). The corresponding ^{13}C shifts (C1 to C6) were assigned via HSQC (Fig. 6B), confirming the identification of ΔGlcA (Δ).

In the 1.20–1.35 ppm region, corresponding to rhamnose H6, six cross peaks were observed in the COSY spectrum (Fig. 6A). The most intense signal at 1.17 ppm correlated with six ^{1}H resonances, at last linking to the anomeric proton signal at 5.14 ppm, which was assigned to α-Rha3S (α). Similarly, the signal at 1.19 ppm was correlated with the proton signal at 4.92 ppm, corresponding to β-Rha3S (β). The linkage between ΔGlcA and α/β-Rha3S was deduced from the HMBC spectrum (Fig. 6B), where C1 of ΔGlcA correlated with the H4 signals of α/β-Rha3S (3.84 and 3.75 ppm), confirming the presence of disaccharide ΔGlcA-α/β-Rha3S.

Additional cross peaks in the COSY spectrum revealed correlations between signals at 1.34–4.01 ppm, 1.33–3.55 ppm, 1.23–4.03 ppm and 1.24–3.57 ppm. These signals were attributed to other free rhamnose residues (named α'-Rha, β'-Rha, α"-Rha and β"-Rha, respectively), though overlapping signals prevented the complete assignment of all resonances. Two additional cross peaks at 1.29–4.16 ppm and 1.29–3.78 ppm likely corresponded to rhamnose without a free anomeric carbon (R and R').

The anomeric signal at 5.08 ppm correlated in the HSQC spectrum (Fig. 6C) with the ^{13}C signal at 105.40 ppm. Four $^{1}H—^{1}H$ correlations were identified in the COSY spectrum, leading to its assignment as iduronic acid (I), though complete characterization was limited by its low abundance. Another anomeric proton at 4.65 ppm correlated with the ^{13}C signal at 106.1 ppm, consistent with xylose (X).

Based on the known constituting units of ulvan and the specificity of ulvan lyase PLSV_3875 in cleaving GlcA-Rha3S bond, two

tetrasaccharides were hypothesized: ΔGlcA-Rha3S-Xyl-α'/β'-Rha3S and ΔGlcA-Rha3S-IdoA-α'/β'-Rha3S. Assignments of α' and α", β' and β", and R and R' were made according to the chemical shifts reported in the literature (Kopel et al., 2016; Yu et al., 2017).

To further investigate ulvan lyase products, UHPLC-HRMS analysis was also performed. The resulting chromatogram (Fig. S7) highlighted the presence of a main peak consistent with prior studies (Chi et al., 2020; Gao et al., 2019; Xu et al., 2021). This peak was attributed to the disaccharide ΔGlcA-Rha3S due to the presence of the single-charged precursor ion at *m/z* 401.0400 and its $[2M–H]^-$ adduct at *m/z* 803.0870. The MS^2 spectrum of ion at *m/z* 401.0400 displayed product ions at *m/z* 285.0289 (fragment Y_1) and 243.0181 (fragment X_1), confirming its identity (Fig. 7A) (Chi et al., 2020; Yu et al., 2017). A second peak was observed at *m/z* 379.0453 and attributed to a double-charged ion corresponding to the tetrasaccharide ΔGlcA-Rha3S-Xyl-Rha3S. Its MS^2 spectrum showed the fragments at *m/z* 321.0394 and 300.0341, corresponding to fragments X_3 and Y_3, respectively (Fig. 7B) (Yu et al., 2017). Both MS^2 spectra also revealed the occurrence of the fragment at *m/z* 96.9589, which represents the $HOSO_3^-$ ion. Additionally, a peak at *m/z* 803.0858, attributable to the tetrasaccharide ΔGlcA-Rha3S-IdoA-Rha3S, overlapped with the most abundant peak of ΔGlcA-Rha3S present also as dimeric form ($[2M-H]^-$ at 803.0870 *m/z*), preventing confident identification (data not shown). Overall, the mass spectra confirmed the presence of disaccharides and tetrasaccharides in the hydrolyzed sample, in agreement with the NMR results.

Considering the potential biological applications of ulvan oligosaccharides, their degree of polymerization (DP) should be taken into account, as it can influence bioactivity. To our knowledge, no studies have assessed the biological activities of ulvan oligosaccharides of different DP in a comparative manner. However, the method developed in this work could be adapted to produce oligosaccharides tailored to specific purposes. For example, stopping the hydrolysis reaction after 1 h under the optimized conditions generated intermediate products of different molecular weights, as shown by the DOSY spectrum in Fig. S8. This experiment also confirmed the endolytic cleavage mechanism of ulvan lyase (Li, Hu, et al., 2020), suggesting that adjusting reaction time represents a viable strategy to modulate the DP distribution of the hydrolysis products according to desired applications.

4. Conclusions

This work developed and optimized an enzymatic protocol for the production of ulvan oligosaccharides from *Ulva lactuca* L. using the commercial ulvan lyase PLSV_3875, overcoming the limitations of traditional acidic hydrolysis. The enzymatic hydrolysis was optimized to obtain a final product suitable for biological applications by minimizing medium salts content and selecting a biocompatible phosphate buffer at a physiological pH with a low concentration of KCl (which substituted NaCl). This approach increased the relative amount of hydrolyzed ulvan in the final dried sample, and allowed direct use of the products, without downstream time-consuming purification via chromatography.

The proposed protocol yielded predominantly the disaccharide ΔGlcA-Rha3S and the tetrasaccharides ΔGlcA-Rha3S-Xyl-Rha3S and ΔGlcA-Rha3S-IdoA-Rha3S, as shown by the NMR and MS experiments. Furthermore, this study demonstrated the possibility of producing oligosaccharides with a higher degree of polymerization by applying reaction times shorter than 3 h, which may be relevant for specific biological applications.

Furthermore, kinetic characterization revealed PLSV_3875 to be highly efficient and robust, with tolerance to a wide range of pH, ionic strength, temperature, and long-term storage stability. Such features suggest suitability for innovative applications, including enzyme immobilization on suitable matrices for recovery and reuse across multiple cycles, or processing cycles involving transiently unstable reaction conditions. Overall, this protocol represents a rapid, practical, scalable approach for the valorization of *Ulva* biomass, supporting future developments in the food, nutraceutical, and biotechnological sectors.

CRediT authorship contribution statement

Beatrice Zonfrillo: Writing – original draft, Methodology, Investigation, Conceptualization. **Maria Bellumori:** Writing – review & editing, Supervision, Conceptualization. **Eleonora Truzzi:** Writing – review & editing, Methodology, Investigation. **Mohamad Khatib:** Supervision, Investigation. **Paola Faraoni:** Writing – review & editing, Methodology, Investigation. **Davide Bertelli:** Writing – review & editing, Supervision, Resources. **Francesco Ranaldi:** Writing – review & editing, Supervision, Resources, Methodology, Investigation, Conceptualization. **Nadia Mulinacci:** Writing – review & editing, Supervision, Resources, Conceptualization.

Declaration of competing interest

The authors declare that they have no known competing financial interests or personal relationships that could have appeared to influence the work reported in this paper.

Appendix A. Supplementary data

Supplementary data to this article can be found online at https://doi.org/10.1016/j.foodchem.2025.145618.

Data availability

Data will be made available on request.

References

Adrien, A., Bonnet, A., Dufour, D., Baudouin, S., Maugard, T., & Bridiau, N. (2019). Anticoagulant activity of sulfated Ulvan isolated from the green macroalga Ulva rigida. *Marine Drugs, 17*(5). https://doi.org/10.3390/md17050291. article 5.

Araújo, R., & Peteiro, C. (2021). Algae as food and food supplements in Europe. *JRC Publications Repository*. https://doi.org/10.2760/049515

Baltrusch, K. L., Torres, M. D., & Domínguez, H. (2024). Characterization, ultrafiltration, depolymerization and gel formulation of ulvans extracted via a novel ultrasound-enzyme assisted method. *Ultrasonics Sonochemistry, 111*, Article 107072. https://doi.org/10.1016/j.ultsonch.2024.107072

Chen, Y., Wu, W., Ni, X., Farag, M. A., Capanoglu, E., & Zhao, C. (2022). Regulatory mechanisms of the green alga Ulva lactuca oligosaccharide via the metabolomics and gut microbiome in diabetic mice. *Current Research in Food Science, 5*, 1127–1139. https://doi.org/10.1016/j.crfs.2022.07.003

Chi, Y., Li, H., Wang, P., Du, C., Ye, H., Zuo, S., Guan, H., & Wang, P. (2020). Structural characterization of ulvan extracted from Ulva clathrata assisted by an ulvan lyase. *Carbohydrate Polymers, 229*, Article 115497. https://doi.org/10.1016/j.carbpol.2019.115497

Chiellini, F., & Morelli, A. (2011). Ulvan: A versatile platform of biomaterials from renewable resources. In R. Pignatello (Ed.), *Biomaterials—physics and chemistry. InTech*. https://doi.org/10.5772/24901

De Ruiter, G. A., Schols, H. A., Voragen, A. G. J., & Rombouts, F. M. (1992). Carbohydrate analysis of water-soluble uronic acid-containing polysaccharides with high-performance anion-exchange chromatography using methanolysis combined with TFA hydrolysis is superior to four other methods. *Analytical Biochemistry, 207*(1), 176–185. https://doi.org/10.1016/0003-2697(92)90520-H

Flórez-Fernández, N., Rodríguez-Coello, A., Latire, T., Bourgougnon, N., Torres, M. D., Buján, M., … Domínguez, H. (2023). Anti-inflammatory potential of ulvan. *International Journal of Biological Macromolecules, 253*, Article 126936. https://doi.org/10.1016/j.ijbiomac.2023.126936

Fournière, M., Latire, T., Lang, M., Terme, N., Bourgougnon, N., & Bedoux, G. (2019). Production of active poly- and Oligosaccharidic fractions from Ulva sp. By combining enzyme-assisted extraction (EAE) and depolymerization. *Metabolites, 9*(9), 182. https://doi.org/10.3390/metabo9090182

Gao, J., Du, C., Chi, Y., Zuo, S., Ye, H., & Wang, P. (2019). Cloning, expression, and characterization of a new PL25 family Ulvan Lyase from marine bacterium Alteromonas sp. A321. *Marine Drugs, 17*(10), 568. https://doi.org/10.3390/md17100568

Hayden, H. S., Blomster, J., Maggs, C. A., Silva, P. C., Stanhope, M. J., & Waaland, J. R. (2003). Linnaeus was right all along: Ulva and Enteromorpha are not distinct genera. *European Journal of Phycology, 38*(3), 277–294. https://doi.org/10.1080/1364253031000136321

Jagtap, A. S., Parab, A. S., Manohar, C. S., & Kadam, N. S. (2022). Prebiotic potential of enzymatically produced ulvan oligosaccharides using ulvan lyase of Bacillus subtilis,

NIOA181, a macroalgae-associated bacteria. *Journal of Applied Microbiology, 133*(5), 3176–3190. https://doi.org/10.1111/jam.15775

Kidgell, J. T., Glasson, C. R. K., Magnusson, M., Sims, I. M., Hinkley, S. F. R., De Nys, R., & Carnachan, S. M. (2024). Ulvans are not equal—Linkage and substitution patterns in ulvan polysaccharides differ with Ulva morphology. *Carbohydrate Polymers, 333*, Article 121962. https://doi.org/10.1016/j.carbpol.2024.121962

Kidgell, J. T., Magnusson, M., De Nys, R., & Glasson, C. R. K. (2019). Ulvan: A systematic review of extraction, composition and function. *Algal Research, 39*, Article 101422. https://doi.org/10.1016/j.algal.2019.101422

Konasani, V. R., Jin, C., Karlsson, N. G., & Albers, E. (2018). Ulvan lyase from Formosa agariphila and its applicability in depolymerisation of ulvan extracted from three different Ulva species. *Algal Research, 36*, 106–114. https://doi.org/10.1016/j.algal.2018.10.016

Kopel, M., Helbert, W., Belnik, Y., Buravenkov, V., Herman, A., & Banin, E. (2016). New family of Ulvan Lyases identified in three isolates from the Alteromonadales order. *Journal of Biological Chemistry, 291*(11), 5871–5878. https://doi.org/10.1074/jbc.M115.673947

Kumar, C. G., Sripada, S., & Poornachandra, Y. (2018). Chapter 14—Status and future prospects of Fructooligosaccharides as nutraceuticals. In A. M. Grumezescu, & A. M. Holban (Eds.), *Role of materials science in food bioengineering* (pp. 451–503). Academic Press. https://doi.org/10.1016/B978-0-12-811448-3.00014-0.

Lahaye, M. (1998). NMR spectroscopic characterisation of oligosaccharides from two Ulva rigida ulvan samples (Ulvales, Chlorophyta) degraded by a lyase. *Carbohydrate Research, 314*(1–2), 1–12. https://doi.org/10.1016/s0008-6215(98)00293-6

Li, C., Tang, T., Du, Y., Jiang, L., Yao, Z., Ning, L., & Zhu, B. (2023). Ulvan and Ulva oligosaccharides: A systematic review of structure, preparation, biological activities and applications. *Bioresources and Bioprocessing, 10*(1), 66. https://doi.org/10.1186/s40643-023-00690-z

Li, J., Chi, Z., Yu, L., Jiang, F., & Liu, C. (2017). Sulfated modification, characterization, and antioxidant and moisture absorption/retention activities of a soluble neutral polysaccharide from *Enteromorpha prolifera*. *International Journal of Biological Macromolecules, 105*, 1544–1553. https://doi.org/10.1016/j.ijbiomac.2017.03.157

Li, Q., Hu, F., Zhu, B., Ni, F., & Yao, Z. (2020). Insights into ulvan lyase: Review of source, biochemical characteristics, structure and catalytic mechanism. *Critical Reviews in Biotechnology, 40*(3), 432–441. https://doi.org/10.1080/07388551.2020.1723486

Li, Y., Ye, H., Wang, T., Wang, P., Liu, R., Li, Y., … Zhang, J. (2020). Characterization of low molecular weight sulfate Ulva polysaccharide and its protective effect against IBD in mice. *Marine Drugs, 18*(10), 499. https://doi.org/10.3390/md18100499

Liu, D., Ouyang, Y., Chen, R., Wang, M., Ai, C., El-Seedi, H. R., … Zhao, C. (2022). Nutraceutical potentials of algal ulvan for healthy aging. *International Journal of Biological Macromolecules, 194*, 422–434. https://doi.org/10.1016/j.ijbiomac.2021.11.084

Lombard, V., Golaconda Ramulu, H., Drula, E., Coutinho, P. M., & Henrissat, B. (2014). The carbohydrate-active enzymes database (CAZy) in 2013. *Nucleic Acids Research*. https://doi.org/10.1093/nar/gkt1178, 42(Database issue), D490-495.

Ning, L., Yao, Z., & Zhu, B. (2022). Ulva (Enteromorpha) polysaccharides and oligosaccharides: A potential functional food source from green-tide-forming macroalgae. *Marine Drugs, 20*(3), 202. https://doi.org/10.3390/md20030202

Nyvall Collén, P., Sassi, J.-F., Rogniaux, H., Marfaing, H., & Helbert, W. (2011). Ulvan Lyases isolated from the Flavobacteria Persicivirga ulvanivorans are the first members of a new polysaccharide Lyase family. *Journal of Biological Chemistry, 286*(49), 42063–42071. https://doi.org/10.1074/jbc.M111.271825

Pérez-Burillo, S., Molino, S., Navajas-Porras, B., Valverde-Moya, Á. J., Hinojosa-Nogueira, D., López-Maldonado, A., … Rufián-Henares, J.Á. (2021). An in vitro batch fermentation protocol for studying the contribution of food to gut microbiota composition and functionality. *Nature Protocols, 16*(7), 3186–3209. https://doi.org/10.1038/s41596-021-00537-x

Qin, H.-M., Gao, D., Zhu, M., Li, C., Zhu, Z., Wang, H., … Lu, F. (2020). Biochemical characterization and structural analysis of ulvan lyase from marine Alteromonas sp. reveals the basis for its salt tolerance. *International Journal of Biological Macromolecules, 147*, 1309–1317. https://doi.org/10.1016/j.ijbiomac.2019.10.095

Qin, H.-M., Xu, P., Guo, Q., Cheng, X., Gao, D., Sun, D., Zhu, Z., & Lu, F. (2018). Biochemical characterization of a novel ulvan lyase from Pseudoalteromonas sp. Strain PLSV. *RSC Advances, 8*(5), 2610–2615. https://doi.org/10.1039/C7RA12294B

Reisky, L., Stanetty, C., Mihovilovic, M. D., Schweder, T., Hehemann, J.-H., & Bornscheuer, U. T. (2018). Biochemical characterization of an ulvan lyase from the marine flavobacterium Formosa agariphila KMM 3901T. *Applied Microbiology and Biotechnology, 102*(16), 6987–6996. https://doi.org/10.1007/s00253-018-9142-y

Rodrigues, V. J., Jouanneau, D., Fernandez-Fuentes, N., Onime, L. A., Huws, S. A., Odaneth, A. A., & Adams, J. M. M. (2024). Biochemical characterisation of a PL24 ulvan lyase from seaweed-associated Vibrio sp. FNV38. *Journal of Applied Phycology, 36*(2), 697–711. https://doi.org/10.1007/s10811-023-03136-3

Shalaby, M., & Amin, H. (2019). Potential using of Ulvan polysaccharide from Ulva lactuca as a prebiotic in Synbiotic yogurt production. *Journal of Probiotics & Health, 07*(01). https://doi.org/10.35248/2329-8901.19.7.208

Tang, T., Cao, S., Zhu, B., & Li, Q. (2021). Ulvan polysaccharide-degrading enzymes: An updated and comprehensive review of sources category, property, structure, and applications of ulvan lyases. *Algal Research, 60*, Article 102477. https://doi.org/10.1016/j.algal.2021.102477

Wichard, T. (2023). From model organism to application: Bacteria-induced growth and development of the green seaweed Ulva and the potential of microbe leveraging in algal aquaculture. *Seminars in Cell & Developmental Biology, 134*, 69–78. https://doi.org/10.1016/j.semcdb.2022.04.007

Xu, F., Dong, F., Sun, X.-H., Cao, H.-Y., Fu, H.-H., Li, C.-Y., … Chen, X.-L. (2021). Mechanistic insights into substrate recognition and catalysis of a new Ulvan Lyase of polysaccharide Lyase family 24. *Applied and Environmental Microbiology*. https://doi.org/10.1128/AEM.00412-21

Yu, Y., Li, Y., Du, C., Mou, H., & Wang, P. (2017). Compositional and structural characteristics of sulfated polysaccharide from Enteromorpha prolifera. *Carbohydrate Polymers, 165*, 221–228. https://doi.org/10.1016/j.carbpol.2017.02.011

Zonfrillo, B., Bellumori, M., Digiglio, I., Innocenti, M., Orlandini, S., Furlanetto, S., … Mulinacci, N. (2025). Multivariate optimization of ulvan extraction applying response surface methodology (RSM): The case of *Ulva lactuca* L. from Orbetello lagoon. *Carbohydrate Polymers, 354*, Article 123340. https://doi.org/10.1016/j.carbpol.2025.123340